

Collective dynamics of liquid HCl: The density–density and longitudinal current correlations

U. Balucani

Istituto di Elettronica Quantistica, Consiglio Nazionale delle Ricerche, I-50127 Firenze, Italy

D. Pasqualini, G. Garberoglio, and R. Vallauri^{a)}

Istituto Nazionale per la Fisica della Materia and Dipartimento di Fisica, Università di Trento, I-38050 Povo, Trento, Italy

G. Sutmann

Research Center Jülich, Central Institute for Applied Mathematics, D-52425, Jülich, Germany

(Received 8 January 2002; accepted 4 October 2002)

In this work the dynamics of density fluctuations in liquid HCl is investigated by computer simulation experiments, with the main goal of ascertaining the influence of hydrogen bonding in the features of the collective excitations of this molecular fluid. The data analysis shows that in HCl the hydrogen bonding has quite a small relevance on the dynamics, in strong contrast with the findings reported for both HF and water. Within the framework of generalized hydrodynamics we have been able to derive values for otherwise unknown quantities like the ratio of specific heats and the adiabatic sound velocity. An evaluation of the average effective interaction potential between the molecular centers of mass, clarifies the interpretation of the collective dynamical behavior explored in the present investigation. © 2003 American Institute of Physics. [DOI: 10.1063/1.1524620]

I. INTRODUCTION

In a recent paper¹ we have reported the results obtained by molecular dynamics computer simulation (CS) of the collective transverse current of liquid HCl. The main purpose of that work was to understand the role played by the hydrogen bonding on the dynamical properties of this weakly associated liquid. The analysis of the transverse current correlation functions and their associated spectra was performed in terms of the corresponding memory functions. The results were compared with those obtained for both strong hydrogen bonded systems (e.g., water and HF) and, on the opposite side, simple monatomic liquids (such as the Lennard-Jones ones).

From both the experimental² and CS (Refs. 3 and 4) side, it was demonstrated that on a length scale of the order of first neighbors distances, peculiar collective excitations can be sustained in both H₂O and HF, due to the local order induced by the hydrogen bonding (tetrahedral in the case of water and zig–zag chainlike in the case of HF). Such excitations appear, at wave vectors larger than a characteristic value, in the spectra of the longitudinal currents as a nondispersive peak, separated from the one due to the presence of propagating density fluctuations (sound peak), as well as in the transverse current spectra. In water at normal conditions, this extra peak occurs at $\omega \approx 10$ rad/ps when the wave vector k exceeds 1 \AA^{-1} . Its origin is traced back to the $\text{O} \cdots \text{O} \cdots \text{O}$ bending motion of three neighboring molecules.^{5–7}

In the case of HF the extra peak occurs at $\omega \approx 50$ rad/ps, i.e., a frequency higher than that corresponding

to the sound peak at about the same wave vector. It has been shown that its appearance stems from the hydrogen bonding stretching of a pair of nearest neighbor molecules.^{7,8} These results point out the relevance of hydrogen bonding in connection to the peculiar local order set up in the system depending on the geometrical shape of the molecules. In Ref. 1, the analysis of the transverse current spectra of HCl through a memory function approach revealed that in this system the situation is more similar to the case of simple monatomic liquids. A good fit of the CS spectra could in fact be obtained by the well known viscoelastic approximation for the memory function. The only exception is at wave vectors $k < 0.5 \text{ \AA}^{-1}$, where it is necessary to model the memory function as a sum of two exponentials in order to achieve a good agreement at low frequencies.

Finally we noticed that at wave vectors around $k \approx 2.5 \text{ \AA}^{-1}$ an extra intensity appears in the transverse current spectra at frequencies around $\omega = 18$ rad/ps, which cannot be accounted for by any simple model. In order to understand whether this feature can be ascribed to the presence of some localized motion of hydrogen bonded molecules (as is the case in water and HF), we have analyzed the wave vector dependence of the density fluctuation and longitudinal current time correlation functions and the corresponding spectra. In the present paper we report the results of such a CS investigation and draw some conclusions on the effect of hydrogen bonding in determining the dynamical behavior of liquids. The format of this paper is as follows. In Sec. II we briefly report the details of the molecular dynamics simulation and introduce the dynamical quantities we will be concerned with. The data are reported and discussed in Sec. III. Finally, Sec. IV summarizes the main conclusions.

^{a)}Author to whom correspondence should be addressed. Electronic mail: vallauri@science.unitn.it

II. COMPUTER SIMULATION DETAILS AND DYNAMICAL QUANTITIES

For the simulation of HCl we have used the C* potential model developed by Klein and McDonald,⁹ which is found to reproduce reasonably well the thermodynamic properties of the liquid as well as the essential features of the experimental structure factors.^{10,11} In the model the molecule is rigid, with the distance between Cl and H atoms fixed at $d = 1.275$ Å. The potential accounts for a Born–Mayer repulsive interaction between like atoms and a damped dispersion series between pairs of Cl atoms. The nondispersive interaction between Cl and H atoms has the effect of stabilizing the bent dimer and it is introduced as a crude attempt to include hydrogen bonding. More specifically,

$$\begin{aligned} U_{\text{HH}}(r) &= 9200 \exp(2.725r), \\ U_{\text{ClH}}(r) &= 2.05 \{ \exp[4.8(r - 2.56)] \\ &\quad - 2 \exp[2.4(r - 2.56)] \}, \\ U_{\text{ClCl}}(r) &= 32.6 \cdot 10^5 \exp(3.8r) \\ &\quad - f(r) \left(\frac{7420}{r^6} + \frac{5.56 \cdot 10^4}{r^8} + \frac{4.75 \cdot 10^5}{r^{10}} \right), \end{aligned} \quad (1)$$

where energies are expressed in kJ/mol and distances in Å and where

$$\begin{aligned} f(r) &= \exp\left(-\frac{5.5-r}{2}\right) r < 5.5 \\ &= 1 \quad r \geq 5.5. \end{aligned} \quad (2)$$

Electrostatic interactions are taken into account through a distributed point charge model. A charge $+Q = 0.592|e|$ is placed on the H and Cl atoms and a charge $-2Q$ on a site along the bond at a distance 0.455 Å from the Cl atom. In order to account for the long range contribution to the electrostatic interactions, the reaction field method was applied. The molecular dynamics simulations were performed at a mass density $\rho = 1.186$ g/cm³ and at an average temperature $\langle T \rangle = 201$ K, on a system of 512 molecules in a cubic box with periodic boundary conditions. Then the box length turns out to be $L = 26.691$ Å and consequently the minimum accessible wave vector is $k_{\min} = 2\pi/L = 0.212$ Å⁻¹. In order to achieve a good energy conservation during the CS runs the time step of integration was fixed at $dt = 2$ fs. Runs as long as 500 000 time steps were carried out to obtain a good statistical accuracy for the evaluated correlation functions. The dynamical variables we are interested in are the wave vector-dependent number density,

$$n(\mathbf{k}, t) = \sum_{i=1}^N \exp(i\mathbf{k} \cdot \mathbf{r}_i(t)) \quad (3)$$

and the longitudinal current

$$j_L(\mathbf{k}, t) = \sum_{i=1}^N [\hat{\mathbf{k}} \cdot \mathbf{v}_i(t)] \exp(i\mathbf{k} \cdot \mathbf{r}_i(t)), \quad (4)$$

where $\mathbf{r}_i(t)$ and $\mathbf{v}_i(t)$ represent the position and the velocity of the center-of-mass of the i th molecule and $\hat{\mathbf{k}}$ is the unit

vector in the direction \mathbf{k} . The correlation functions relative to these two variables are the intermediate scattering function,

$$F(k, t) = \frac{1}{N} \langle n^*(\mathbf{k}, 0) n(\mathbf{k}, t) \rangle \quad (5)$$

and the longitudinal current correlation function

$$C_L(k, t) = \frac{1}{N} \langle j_L^*(\mathbf{k}, 0) j_L(\mathbf{k}, t) \rangle, \quad (6)$$

respectively.

In order to evaluate the errors on the spectra we have used an autoregressive (AR) model to represent the simulation data.¹² In this model a random process is generated according to

$$x_n = \sum_{k=1}^p a_k x_{n-k} + \xi_n, \quad (7)$$

where a_k are constants, ξ_n are independent Gaussian random variables with zero mean and variance σ^2 . The parameters of the model are chosen so that the spectrum of the random process is as close as possible to the spectrum of the quantity of interest.

III. COMPUTER SIMULATION RESULTS

The dynamical structure factors, $S(k, \omega)$, obtained by a Fourier transform of the intermediate scattering functions $F(k, t)$, are reported for a series of wave vectors in Fig. 1.

We notice that the maximum error occurs at a frequency $\omega = 0$, and its relative magnitude is of the order of $\Delta_S = 6\%$.

At the first two reported wave vectors, a pronounced shoulder at finite frequencies is apparent, indicating the presence of damped sound waves even at wavelengths comparable with nearest neighbor distances. The situation is similar to the one found experimentally^{13,14} and by CS (Ref. 15) for liquid alkali metals, even if in this case a well defined peak appears which persists to comparatively larger wave vectors. In the case of HCl, as k increases, the shoulder becomes broader and broader, thus indicating that the sound wave is overdamped, and eventually disappears.

To follow the k -dependence of the inelastic features, rather than $S(k, \omega)$, one usually considers the spectra of the longitudinal currents, shown in Fig. 2 at the same wave vectors.

We notice that the maximum error occurs at the frequency where the spectrum has its maximum, and its relative magnitude is of the order of $\Delta_C = 4\%$.

The resulting values of the peak frequency $\omega_p(k)$ are shown in Fig. 3. Dividing $\omega_p(k)$ by k one obtains an effective sound velocity $v_p(k)$, reported in Fig. 4 along with the corresponding values of the isothermal sound velocity deduced from the expression,

$$c_0(k) = \sqrt{\frac{k_B T}{m S(k)}} \quad (8)$$

and of the “infinite frequency” longitudinal sound velocity,

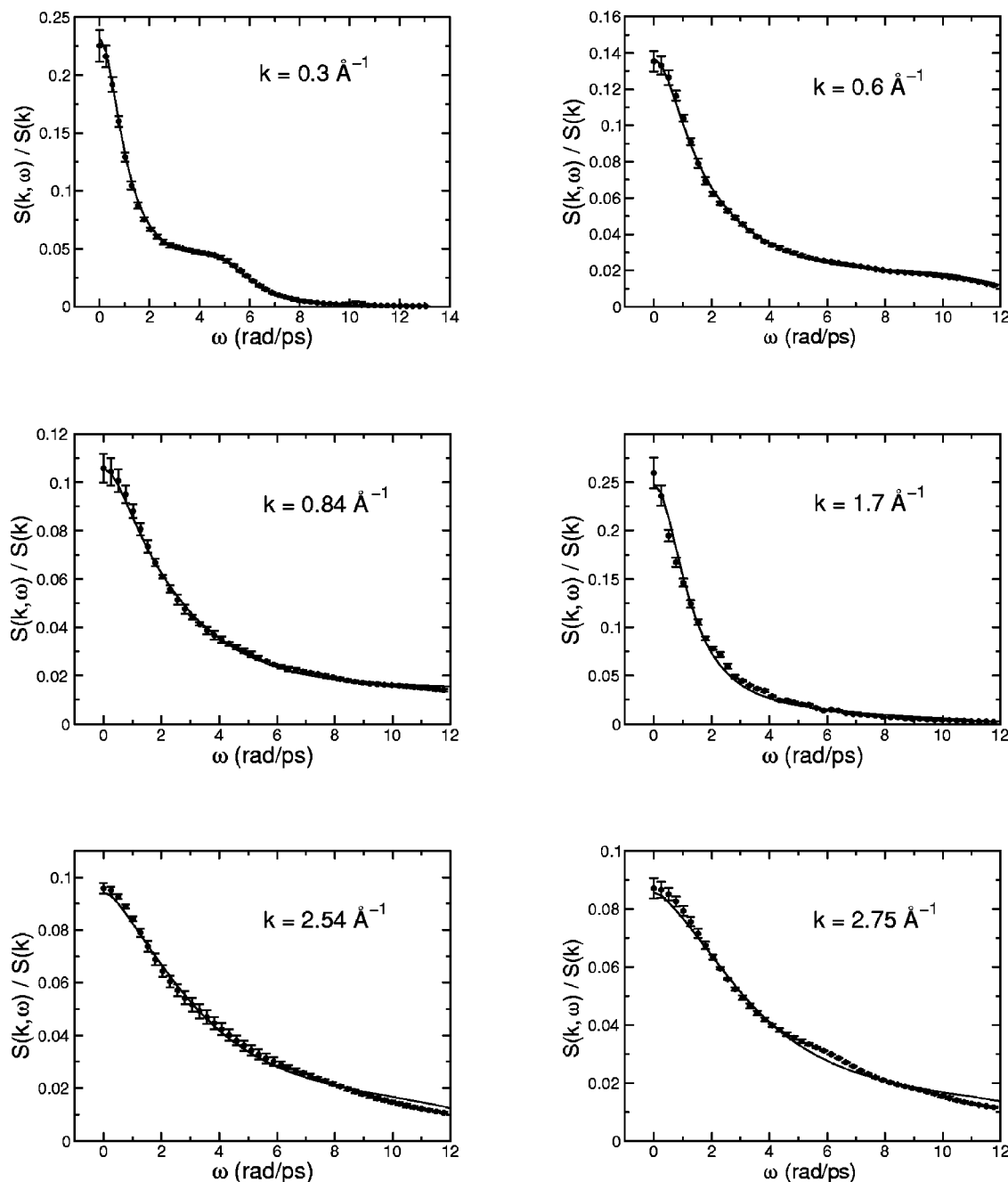


FIG. 1. Dynamical structure factor at different k vectors. Full circles: MD data; solid line: the best fits of viscoelastic model to the MD spectra. The error bars are the results of the AR analysis.

$$c_{\infty}(k) = \frac{\omega_L(k)}{k}. \quad (9)$$

In Eq. (8), $S(k)$ represents the structure factor of the molecular centers-of-mass, m is the total mass of the molecule, whereas in Eq. (9), $\omega_L(k)$ is the normalized second frequency moment of the longitudinal current spectra, obtained from the CS data by fitting the short time behavior of the corresponding functions. Since the ratio of specific heats $\gamma = c_p/c_v$ is not known for pure liquid HCl, it is not possible to derive any value for the adiabatic sound velocity $c_s(k=0) = \sqrt{\gamma}c_0(k=0)$. As shown in the following, the analysis

in terms of generalized hydrodynamics will allow us to estimate γ and consequently a value for the adiabatic sound velocity otherwise unknown.

The picture that emerges from these data is very similar to the one describing the collective dynamical properties of monatomic liquids and in particular of alkali metals. At increasing wave vectors, beyond the hydrodynamic limit, density fluctuations can propagate in HCl with a velocity higher than the isothermal one. These density waves become overdamped for $k > 0.6 \text{ \AA}^{-1}$. This positive sound dispersion accounts for the well known solidlike response of the system

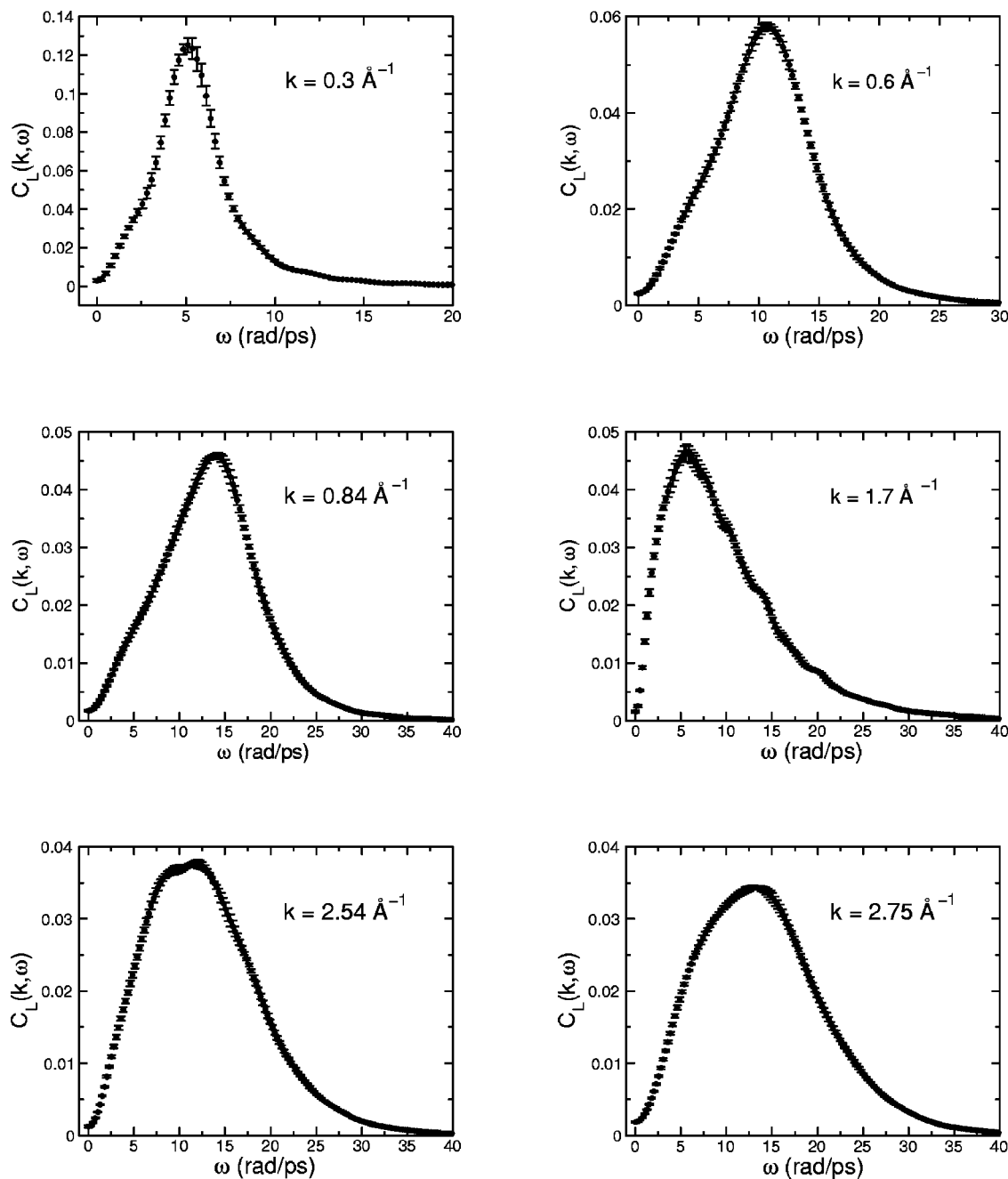


FIG. 2. The spectra of the longitudinal current at different k vectors. The spectra are obtained from $C_L(k, t)$ calculated from MD. The error bars are the result of the AR analysis.

on a length scale of the order of first neighbor distances, where the ordering of the molecules is more pronounced, i.e., close to that of a crystal. By inspection of the longitudinal current spectra, there is no evidence of extra peaks at any investigated wave vector. Therefore the present results do not confirm the observation of a second feature at $k \approx 2.5 \text{ \AA}^{-1}$ as made in the analysis of the transverse current spectra. In this respect, hydrogen bonding appears to have little influence on the dynamical properties of HCl.

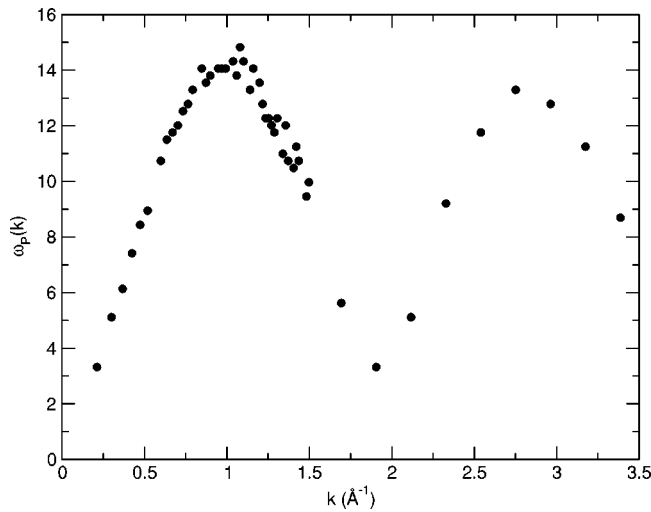
A deeper insight into the physical processes underlying the collective dynamics can be obtained by the memory function approach.¹⁶ In this framework one starts writing the dynamical structure factor in terms of the Laplace transform

of the intermediate scattering function $\hat{F}(k, z)$ as

$$S(k, \omega) = \frac{1}{\pi} \text{Re}[\hat{F}(k, z = i\omega)], \quad (10)$$

$\hat{F}(k, z)$ can be expressed in terms of its second order memory function $\hat{K}_L(k, z)$,

$$\hat{F}(k, z) = \frac{S(k)}{z + \frac{\langle \omega_k^2 \rangle}{z + \hat{K}_L(k, z)}}, \quad (11)$$

FIG. 3. The k dependence of the $C_L(k, \omega)$ peak position.

where $\langle \omega_k^2 \rangle = c_0^2 k^2$. After some algebra the dynamical structure factor can eventually be written as

$$\frac{S(k, \omega)}{S(k)} = \frac{1}{\pi} \frac{\langle \omega_k^2 \rangle K'_L}{[\omega^2 - \langle \omega_k^2 \rangle - \omega K''_L]^2 + [\omega K'_L]^2}, \quad (12)$$

where K'_L and K''_L are the real and the negative of the imaginary part of $\hat{K}_L(k, z=i\omega)$, respectively. For brevity their k and ω dependence has been omitted.

In order to give a description of $S(k, \omega)$ on a microscopic scale, we have performed a fitting procedure of the CS results with a viscoelastic approximation for the memory function $K_L(k, t)$, as done for the transverse current.¹ However, in contrast with the transverse case, the coupling to the thermal fluctuations has to be taken into account here.¹⁶ Consequently the memory function $K_L(k, t)$ is written as

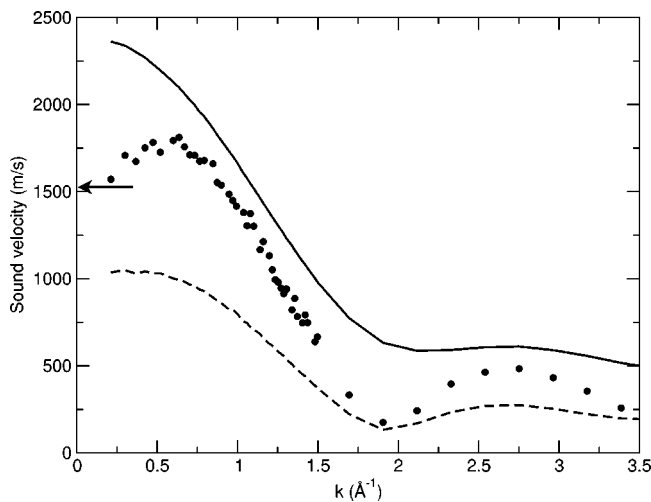


FIG. 4. The k dependent phase velocity $v_p(k) = \omega_p(k)/k$ (full circles), the velocity $c_0(k)$ from Eq. (8) (dashed line) and the “infinite-frequency” longitudinal velocity $c_\infty(k)$ defined in Eq. (9) (solid line). The arrow indicates the value of the adiabatic sound velocity $c_s = \sqrt{\gamma}c_0$, obtained by extrapolating $\gamma(k)$ and $c_0(k)$ at $k=0$.

$$K_L(k, t) = [\omega_L^2(k) - \gamma(k)\langle \omega_k^2 \rangle] \exp[-t/\tau(k)] + (\gamma(k) - 1)\langle \omega_k^2 \rangle \exp[-tA(k)k^2]. \quad (13)$$

Equation (13) guarantees that all the moments of $S(k, \omega)$ are correct up to the fourth. It extends the hydrodynamic result at finite wave vectors, by introducing the k -dependent coefficients $\gamma(k)$ and $A(k)$, which in the limit of $k \rightarrow 0$ coincide with the ratio of specific heats and the thermal diffusivity, respectively. The first term in Eq. (13) accounts for the “viscous” relaxation mechanisms of the density fluctuations through the single relaxation time $\tau(k)$, whereas the second one accounts for the relaxation of temperature fluctuations. This term becomes ineffective when $\gamma(k)$ approaches unity, as is the case for alkali metals and even water. In our fitting procedure $\gamma(k)$, $\tau(k)$, and $A(k)$ are free parameters to be adjusted to obtain the best reproduction of the CS data for the dynamical structure factor. An extrapolation at $k \rightarrow 0$ will provide an estimate of γ .

For the sake of completeness we report also the expressions for K'_L and K''_L which result from the model, Eq. (13),

$$K'_L(k, \omega) = \frac{[\omega_L^2(k) - \gamma(k)\langle \omega_k^2 \rangle]/\tau(k)}{\omega^2 + \tau^{-2}(k)} + \frac{(\gamma(k) - 1)\langle \omega_k^2 \rangle A(k)k^2}{\omega^2 + (A(k)k^2)^2}, \quad (14)$$

$$K''_L(k, \omega) = \omega \left[\frac{\omega_L^2(k) - \gamma(k)\langle \omega_k^2 \rangle}{\omega^2 + \tau^{-2}(k)} + \frac{(\gamma(k) - 1)\langle \omega_k^2 \rangle}{\omega^2 + (A(k)k^2)^2} \right].$$

The insertion of Eqs. (14) into Eq. (12) allows us to write the dynamical structure factor in terms of the parameters of the model.

In order to obtain reasonable values for the parameters (e.g., avoiding negative values of γ) a careful fitting procedure has to be performed. Since there are only three free parameters it is possible to scan the whole parameter space bound to certain maximum and minimum values of $\tau(k)$, $A(k)$, and $\gamma(k)$ and choose those parameters for which a χ^2 estimate gives the best approximation to the curve from the CS results. For example, an initial value for $\tau(k)$ was chosen close to the value which gave the best fitting for the transverse current spectra within the same single relaxation time approximation. The results are summarized in Figs. 5, 6, and 7 for $\tau(k)$, $A(k)$, and $\gamma(k)$, respectively. The shapes of $S(k, \omega)$ obtained with the best fitting parameters are reported in Fig. 1 along with the CS data. It appears evident that the agreement is very good in the whole range of reported wave vectors, the only discrepancy being the fact that the model tends to overemphasize the presence of propagating density waves. In fact a tiny little bump is still present in the spectra at a wavevector as large as 2.54 \AA^{-1} , in contrast to what it is apparent from the CS data. In Fig. 5 the values of the rate $1/\tau(k)$ are compared with the corresponding ones found in the fitting procedure of the transverse current spectra by a viscoelastic model.¹ The fact that these relaxation rates turn out to be close to each other parallels similar results obtained in Lennard-Jones liquids.¹⁷ It is interesting to note that the coefficient $\gamma(k)$ decreases rapidly to unity with increasing k , thus making the coupling between density and energy fluc-

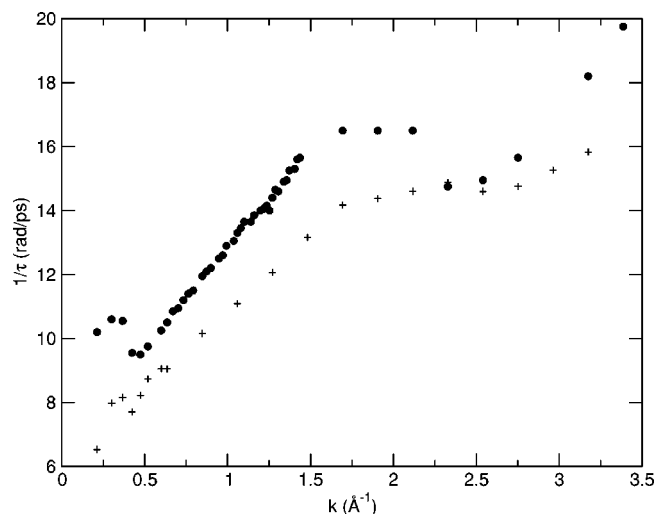


FIG. 5. The viscoelastic relaxation rate deduced from the best fit of the viscoelastic approximation to $S(k, \omega)$ (full circle) and the viscoelastic relaxation rate deduced from the fit of the transverse current (cross).

tuations virtually negligible at wave vectors of the order of 1.0 \AA^{-1} . An extrapolation of these data at $k \rightarrow 0$ leads to a value of $\gamma = 2.4 \pm 0.1$.

The similarities of these results with what is known for the collective dynamical behavior of monatomic liquids (alkali metals or Lennard-Jones systems) suggest an investigation as to which extent an effective potential between two molecules resembles the interaction potential acting between two particles in an atomic liquid. As already mentioned the full potential energy is the sum of site-site terms, i.e., those reported in Eq. (1) plus the Coulomb electrostatic contributions.

If $V(\mathbf{R}_1, \mathbf{R}_2, \Omega_1, \Omega_2)$ is the full interaction potential between molecule 1 at position \mathbf{R}_1 with orientation Ω_1 and molecule 2 at position \mathbf{R}_2 with orientation Ω_2 , we have evaluated the integral,

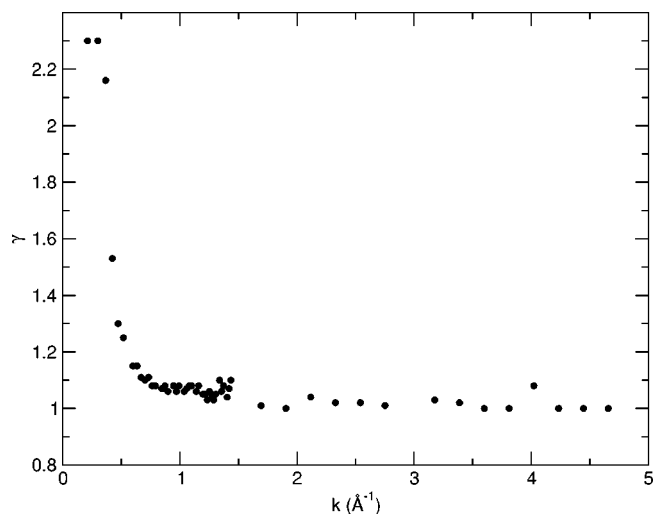


FIG. 7. The k dependence of the ratio of the specific heat $\gamma(k)$.

$$v(|\mathbf{R}_1 - \mathbf{R}_2|) = \frac{1}{(4\pi)^2} \int V(\mathbf{R}_1, \mathbf{R}_2, \Omega_1, \Omega_2) d\Omega_1 d\Omega_2. \quad (15)$$

The results of this calculation are reported in Fig. 8, which also shows a Lennard-Jones potential having the same well depth and position of the minimum as the calculated one. This effective potential turns out to be slightly less repulsive at short separations and to decrease less rapidly than the Lennard-Jones one at larger distances. A separation of the potential into an electrostatic and a nonelectrostatic contribution (reported in the inset of Fig. 8) gives some insight into the importance of hydrogen bonding. Assuming that this feature is present mainly due to the electrostatic terms in the potential, it is seen that the minimum of the potential is shifted to smaller distances due to electrostatics. This is a direct evidence that the hydrogen-bond tends to decrease the interparticle distance from ~ 4.1 to $\sim 3.9 \text{ \AA}$. As is also found, the depth of the potential is drastically decreased from $\sim 1 \text{ kJ/mol}$ (a value close to the one for argon) to $\sim 4 \text{ kJ/mol}$, which stabilizes neighbored particle associations.

Moreover the potential does not present any oscillation around zero at long distances, in contrast with the behavior of the pseudopotential adopted for alkali metals. As far as the density effect on the liquid structure this effective potential leads to a behavior again similar to simple monatomic systems; in fact the number of first nearest neighbors turns out to be close to eleven in the thermodynamic state explored in the present work. Since the center-of-mass pair distribution function of HCl is close to the one of a Lennard-Jones liquid, one is tempted to conclude that even the collective dynamical features are similar. The present analysis of the density and longitudinal current correlations as well as the previous study of the transverse case indeed supports such an expectation.

IV. CONCLUSIONS

The present analysis of the collective dynamics of liquid HCl, at the level of density fluctuations and longitudinal cur-

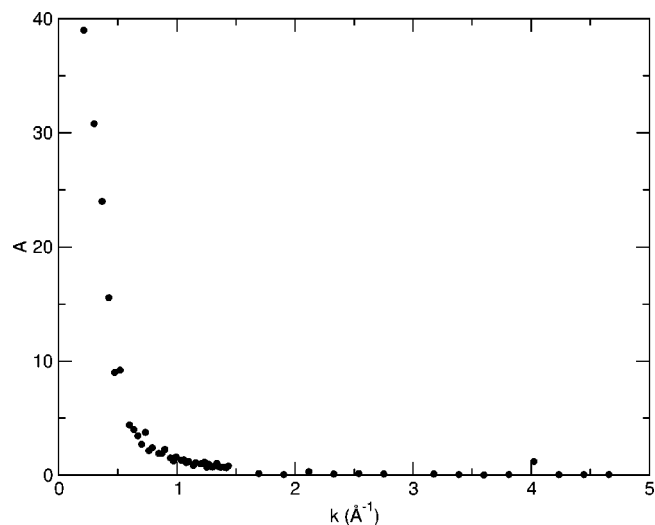


FIG. 6. $A(k)$ from the best fit of the viscoelastic approximation to $S(k, \omega)$.

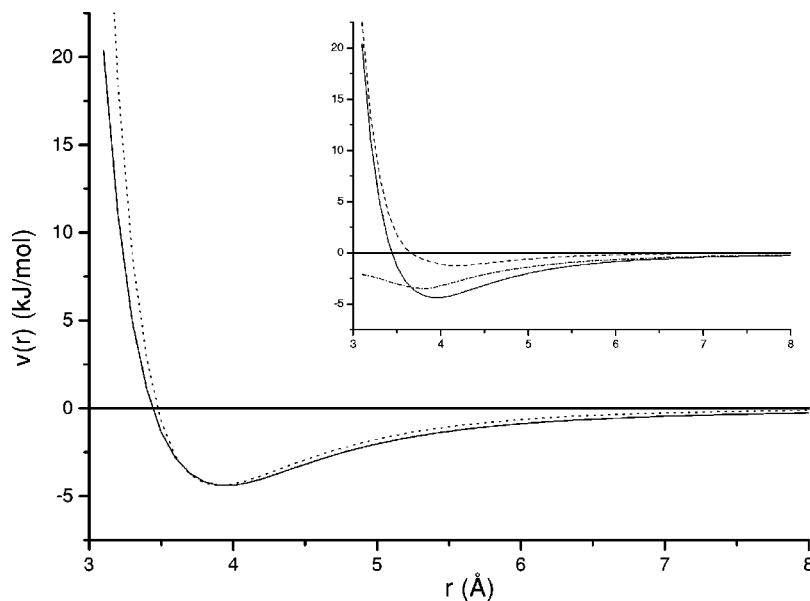


FIG. 8. The average potential $v(r)$ of Eq. (15) (solid line) and a Lennard-Jones potential with the same depth and minimum position of $v(r)$ (dotted line). The inset shows the separation into electrostatic (dotted-dashed line) and nonelectrostatic contribution (dashed line).

rents, has clarified some unclear aspects of this weakly hydrogen bonded system. First of all, contrary to what could be deduced from the observation of the transverse current spectra, the longitudinal ones do not show any evidence of extra peaks appearing at some peculiar wave vector. At this level one can therefore exclude any strong influence of hydrogen bonding in characterizing the collective dynamics. Secondly, the analysis of density fluctuations by the memory function formalism has shown that the standard approximations adopted for monatomic liquids lead to a satisfactory reproduction of the spectral shapes. However, it is essential to account for the coupling to thermal fluctuations through an wave vector dependent specific heat ratio $\gamma(k)$. By the fitting procedure we were able to derive values for $\gamma(k)$ which, when extrapolated to $k=0$, allowed to estimate γ and consequently the adiabatic sound velocity, otherwise unknown.

In HCl propagating density waves are found to be well defined up to $k_0 = 0.6 \text{ \AA}^{-1}$, i.e., $\approx 0.34 k_m$, where $k_m = 1.76 \text{ \AA}^{-1}$ represents the position of the main peak of $S(k)$. In this respect HCl behaves in an intermediate way between molten alkali metals ($k_0/k_m \approx 0.76$) and Lennard-Jones liquids ($k_0/k_m \approx 0.15$). As pointed out by Lewis and Lovesey,¹⁸ this behavior can be associated with the more or less symmetrical shape of the potential well near the minimum. The calculation of an effective two body interaction potential energy between two molecules has indeed revealed that this function turns out to be less steep at short and to decay to zero less rapidly at long distances; a result in agreement with the Lewis and Lovesey conjecture.

ACKNOWLEDGMENTS

This work has been partially supported by the German Italian Vigoni program of DAAD and CRUI.

- ¹U. Balucani, D. Pasqualini, G. Sutmann, and R. Vallauri, J. Chem. Phys. **114**, 8467 (2001).
- ²F. Sette, G. Ruocco, M. Krisch, U. Bergmann, C. Masciovecchio, V. Mazzacurati, G. Signorelli, and R. Verbeni, Phys. Rev. Lett. **75**, 850 (1995).
- ³U. Balucani, G. Ruocco, A. Torcini, and R. Vallauri, Phys. Rev. E **47**, 1677 (1993).
- ⁴D. Bertolini, G. Sutmann, A. Tani, and R. Vallauri, Phys. Rev. Lett. **81**, 2080 (1998).
- ⁵F. Sciortino and S. Sastry, J. Chem. Phys. **100**, 3881 (1994).
- ⁶G. Sutmann and R. Vallauri, J. Phys.: Condens. Matter **10**, 9231 (1998).
- ⁷G. Garberoglio, G. Sutmann, and R. Vallauri, J. Chem. Phys. **117**, 3278 (2002).
- ⁸G. Garberoglio and R. Vallauri, Phys. Rev. Lett. **84**, 4878 (2000), cond-mat/0001265.
- ⁹L. M. Klein and I. R. McDonald, Mol. Phys. **42**, 243 (1981).
- ¹⁰A. K. Soper and P. Egelstaff, Mol. Phys. **42**, 399 (1981).
- ¹¹C. Andreani, M. Ricci, M. Nardone, F. Ricci, and A. K. Soper, J. Chem. Phys. **107**, 214 (1997).
- ¹²G. Box and G. Jenkins, *Time Series Analysis: Forecasting and Control* (Holden-Day, San Francisco, 1976).
- ¹³J. R. D. Copley and J. M. Rowe, Phys. Rev. Lett. **32**, 49 (1974).
- ¹⁴D. Pasqualini, R. Vallauri, Chr. Morkel, F. Demmel, and U. Balucani, J. Non-Cryst. Solids **250–252**, 76 (1999).
- ¹⁵A. Rahman, Phys. Rev. Lett. **9**, 1667 (1974).
- ¹⁶U. Balucani and M. Zoppi, *Dynamics of the Liquid State* (Oxford Science, Oxford, 1994).
- ¹⁷D. Levesque, L. Verlet, and J. K rkij rvi, Phys. Rev. A **7**, 1690 (1973).
- ¹⁸J. W. E. Lewis and S. W. Lovesey, J. Phys. C **10**, 3221 (1977).